



AALBORG UNIVERSITY
DENMARK

Aalborg Universitet

Optimizing the conditions for hydrothermal liquefaction of barley straw for bio-crude oil production using response surface methodology

Zhu, Zhe; Rosendahl, Lasse Aistrup; Toor, Saqib Sohail; Chen, Guanyi

Published in:
Science of the Total Environment

DOI (link to publication from Publisher):
[10.1016/j.scitotenv.2018.02.194](https://doi.org/10.1016/j.scitotenv.2018.02.194)

Creative Commons License
Unspecified

Publication date:
2018

Document Version
Accepted author manuscript, peer reviewed version

[Link to publication from Aalborg University](#)

Citation for published version (APA):
Zhu, Z., Rosendahl, L. A., Toor, S. S., & Chen, G. (2018). Optimizing the conditions for hydrothermal liquefaction of barley straw for bio-crude oil production using response surface methodology. *Science of the Total Environment*, 630, 560-569. <https://doi.org/10.1016/j.scitotenv.2018.02.194>

General rights

Copyright and moral rights for the publications made accessible in the public portal are retained by the authors and/or other copyright owners and it is a condition of accessing publications that users recognise and abide by the legal requirements associated with these rights.

- ? Users may download and print one copy of any publication from the public portal for the purpose of private study or research.
- ? You may not further distribute the material or use it for any profit-making activity or commercial gain
- ? You may freely distribute the URL identifying the publication in the public portal ?

Take down policy

If you believe that this document breaches copyright please contact us at vbn@aub.aau.dk providing details, and we will remove access to the work immediately and investigate your claim.

1 **Optimizing the conditions for hydrothermal liquefaction of barley straw for** 2 **bio-crude oil production using response surface methodology**

3 Zhe Zhu^a, Lasse Rosendahl^b, Saqib Sohail Toor^b, Guanyi Chen^c

4 ^aSchool of Environmental Science and Safe Engineering, Tianjin University of
5 Technology, Tianjin, 300384, PR China

6 ^bDepartment of Energy Technology, Aalborg University, Aalborg, 9220, Denmark

7 ^c School of Environmental Science and Engineering/State Key Laboratory of Engines,
8 Tianjin University, Tianjin, 300072, PR China

9 10 **Abstract:**

11 The present paper examines the conversion of barley straw to bio-crude oil (BO)
12 via hydrothermal liquefaction. Response surface methodology based on central
13 composite design (CCD) was utilized to optimize the conditions of four independent
14 variables including reaction temperature (factor X_1 , 260-340 °C), reaction time (factor
15 X_2 , 5-25 min), catalyst dosage (factor X_3 , 2-18 %) and biomass/water ratio (factor X_4 ,
16 9-21 %) for BO yield. It was found that reaction temperature, catalyst dosage and
17 biomass/water ratio had more remarkable influence than reaction time on BO yield by
18 analysis of variance (ANOVA). The predicted BO yield by the second order
19 polynomial model was in good agreement with experimental results. A maximum BO
20 yield of 38.72 wt% was obtained at 304.8 °C, 15.5 min, 11.7 % potassium carbonate
21 as catalyst and 18% biomass (based on water). GC/MS analysis revealed that the
22 major BO components included phenols and their derivatives, acids, aromatic
23 hydrocarbon, ketones, N-contained compounds and alcohols, which makes it a
24 promising material in the applications of either as a phenol substitute in bio-phenolic
25 resins or bio-fuel.

26 **Key words:** Hydrothermal liquefaction, Barley straw, Central composite design,
27 Response surface methodology

28 **1. Introduction**

29 Nowadays, issues related to energy security, climate change mitigation, and
30 sustainable development enhanced the overall utilization of renewable energy, which
31 is the world's fast-growing energy source. Among them, bioenergy is the largest

32 renewable energy source worldwide, the total supply of which accounted for 10.3% of
33 the global energy supply in 2014. (Kummamuru, 2017). Barley straw, an agricultural
34 residue, represents one of the largest lignocellulosic biomass in Denmark. In 2016,
35 almost 2.17 million tons of barley straw was produced. Unfortunately, 34.12% was
36 left on the field and has not been utilized yet. Only 22.56% was converted to energy
37 through combustion and power generation etc., 29.74% was used as fodder (Denmark,
38 2014). Therefore, there is an urgency to find suitable solutions to convert remaining
39 straw. One of the effective methods for crops straw utilization is biofuel production
40 through fast pyrolysis (Das and Sarmah, 2015; Hsieh et al., 2015; Xu et al., 2017) and
41 hydrothermal liquefaction (HTL) (Gollakota et al., 2017; Midgett et al., 2012; Younas
42 et al., 2017), which is anticipated to provide 27% of global transportation fuels by
43 2050. Most importantly, it is estimated that for OECD countries 2.1 Gton of carbon
44 dioxide in the atmosphere can be reduced every year according to such use of biofuels
45 (IEA, 2012).

46 HTL has gained significant interest in recent years, and has been demonstrated to
47 be competitive with thermochemical routes such as pyrolysis for converting biomass
48 into biofuels due to feedstock flexibility, high energy and resource efficiency of the
49 process and high output product quality (Patel et al., 2016; Suárez-Iglesias et al.,
50 2017). Feedstock flexibility and process efficiency are important factors for the
51 sustainable operation of new biofuel technologies. HTL converts diversified biomass
52 in hot compressed liquid (water/organic solvent) into four different products:
53 bio-crude oil (BO) with higher heating values up to 38 MJ/kg (Toor et al., 2011),
54 aqueous phase containing multiple organic compounds which can be reused in this
55 process (Déniel et al., 2016; Hu et al., 2017; Zhu et al., 2015a) or utilized for
56 cultivation of microalgae afterwards (Hu et al., 2017), solid residues used for heating
57 or as soil amendment (Yu et al., 2017), as well as gaseous products mainly including
58 CO₂ and H₂. In particular, bio-crude oil, a promising alternative energy source with
59 high energy density, has the potential to be used as a liquid fuel in boilers, engines and
60 turbines or chemical feedstocks (Xiu and Shahbazi, 2012). Therefore, HTL of barley
61 straw with emphasis on bio-crude production was conducted in this study.

62 Production of BO from barley straw using HTL technology has been investigated
63 in our previous studies (Zhu et al., 2015a; Zhu et al., 2015b; Zhu et al., 2014) where
64 the single-factor experiments were conducted, and product yield and properties were
65 studied as well. It showed that the maximum BO yield of 34.9 wt% was achieved at
66 300 °C, 10 wt% K₂CO₃ as catalyst, biomass to water ratio of 15% under a fixed
67 retention time of 15 min. In addition, low temperature (<320 °C) and with the addition
68 of K₂CO₃ favor BO yield. Indeed, reaction time and biomass/water ratio influence the
69 product distribution and properties as well (Toor et al., 2011). A number of
70 independent factors were discussed, while the interactions between them were not
71 considered. Therefore the conditions need to be further optimized.

72 Response surface methodology (RSM) is a kind of optimal design for regression
73 model, which is a rapid technique for development, improvement and optimizing
74 process, based on the data from experiments conducted at a set of input variables at
75 multiple levels. It allowed established the significance of each parameter and the
76 significant interaction between parameters. Compared with other experimental design
77 methods, it has the advantage of optimizing nonlinear systems, providing a more
78 precise computation of the main and interaction effects through regression fitting
79 (Diamond, 1981; Eriksson et al., 1996; Hassan et al., 2017). Thus, this method has
80 already been used to optimize process parameters during thermal conversion of
81 different biomass, such as algae, cotton stalk, palm kernel shell etc. (Chan et al., 2017;
82 Li et al., 2017; Liu et al., 2013). Li et al. (Li et al., 2017) optimized three operating
83 parameters (microwave power, reaction temperature and time) during
84 microwave-assisted pyrolysis. Chan et al. (Chan et al., 2017) performed optimization
85 study on HTL of palm kernel shell using RSM with central composite rotation design
86 (CCRD) involving four factors (temperature, pressure, reaction time and biomass to
87 water ratio). Similarly, the CCRD was also employed by Liu et al. (Liu et al., 2013) to
88 find the optimization conditions for HTL of macroalgae by three variables
89 (temperature, catalyst and solvent/biomass ratio). Yet, little research has been
90 conducted to investigate the bio-crude oil production from barley straw through HTL
91 process.

92 This paper moves further to a more systematic study on the effects of four
 93 experimental variables (reaction temperature, reaction time, catalyst dosage,
 94 biomass/water mass ratio) and their interactions on bio-crude oil production based on
 95 the RSM experiment. A central composite design (CCD) experimental design was
 96 employed and the response surface model was analyzed. Finally, the validity of model
 97 was confirmed by conducting numerical examples. More detailed analysis of
 98 chemical properties of BO was performed, to provide a guidance for the design of
 99 utilization of barley straw and the further pilot and industrial scale practice.

100 2. Materials and Methods

101 2.1 Materials and characterization

102 The barley straw was obtained from Denmark. Before experiment, it was
 103 grounded into small particles having a size of less than 1.0 mm and then dried
 104 overnight at 105 °C for 24 hours. The elemental composition is shown in Table 1. The
 105 elemental analysis (CHNS) of biomass was performed with a 2400 Series II CHNS/O
 106 Element analyzer (PerkinElmer, USA). The water content was determined by
 107 calculating the weight loss before and after drying at 105 °C in an oven for at least 12
 108 hours. Higher heating values (HHVs) were measured using C2000 basic Calorimeter
 109 (IKA, German).

110 **Table 1** Elemental composition of raw biomass

Biomass	Elemental content (wt% dry basis)					HHV (MJ/kg)	Ash content (wt%)	Water content (wt%)
	C	H	N	S	O ^a			
Barley straw	44.66	6.34	0.46	0.57	47.97	17.38	4.26	6.21

111 ^a By difference

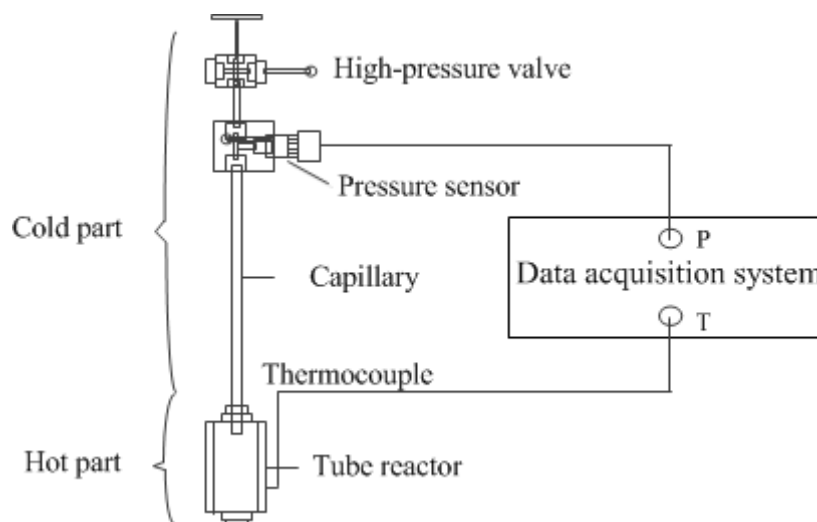
112 Typically, barley straw in Demark consists of cellulose, hemicellulose and lignin
 113 with the content of 46%, 23%, and 15%, respectively (Sander, 1997).

114 The reagent grade acetone was used as rinsing solvent for product separation,
 115 which was purchased from Sigma-Aldrich and used as received. Potassium carbonate
 116 (K₂CO₃) was purchased from Sigma-Aldrich and used as catalyst.

117 2.2 Experiment setup

118 The experiments were carried out in 10 mL micro reactors which were assembled
119 by Swagelok tubes and fittings. The reactor consists of a 200 mm length of SS316
120 tube (12 mm O.D. with a wall thickness of 2 mm) fitted with a Swagelok cap at one
121 end, and the other end was fitted with a capillary connected to a high pressure sensor.
122 The real-temperature and pressure was transferred to the Matlab program through the
123 data acquisition system. A fluidized baths (SBL-2D type with a TC-9D type
124 temperature controller, Techne calibration) with maximum temperature of 600 °C
125 was employed for heating reactors. Fig. 1 shows the schematic diagram of micro
126 reactor. Prior to HTL experiments, we did pressure tests with nitrogen to make sure
127 that the reactors were tightly sealed.

128 In a typical experiment, 6 g distilled water and between 0.54 and 1.26 g barley
129 straw (making biomass concentration of 9-21wt% on a dry basis) was placed in the
130 reactor, with a certain quantity of K_2CO_3 (2-18 wt% of biomass) as well. Then the
131 reactor was sealed and purged with N_2 for three times to ensure that no air was
132 remained inside. Before experiment, the reactors were pressured to 10 bars with N_2 in
133 case of water boiling during heating. Then they were immersed in sand bath fluidized
134 bed preheated to the set temperature and oscillated up and down which is controlled
135 by VLT 2800 Variable-frequency drive. After the reactor reached to reaction
136 temperature, it was hold at that temperature for the required time (5-25 min). Finally,
137 the reactor was cooled down in cold water bath. For each of these conditions, the
138 experiments were conducted in triplicates. The results herein are mean values, and
139 uncertainties are standard deviations.



140
141 **Fig. 1.** Schematic diagram of micro reactor

142 **2.3 Separation of reaction products**

143 The cooled reactors were opened without collecting gaseous products. Since the
144 main attention in this work was paid on the optimization of bio-crude oil production
145 with higher yield and energy contents, gas fraction was thus not collected and
146 analyzed in this work. Similar method was used in the literature (Déniel et al., 2016;
147 Hu et al., 2017; Parsa et al., 2018; Zhang et al., 2009).

148 The liquid product was poured to a beaker and filtered through the Whatman No.
149 5 filter paper to separate the aqueous phase (AP) from solids. Then the reactor, cap
150 and capillary were rinsed with acetone several times to remove any leftover matter
151 including bio-crude oil and solids adhering on them. Afterwards, the mixture
152 containing oil phase, solids and acetone were filtrated and the remaining solids on the
153 filter paper were dried in a furnace at 105 °C for 24 hours and then weighted to
154 determine the solid residues (SR) yield. The acetone and water formed during HTL
155 was removed by a rotary evaporator (Buchi Rotavapor R-210, Switzerland) at a
156 reduced pressure at 60 °C. The dark oil phase left was weighed and referred to as
157 bio-crude oil (BO). The yields of BO and SR were determined on a dry basis by Eqs.
158 (1-2):

159
$$BO \text{ yield (wt\%)} = \frac{\text{mass of BO obtained (g)}}{\text{mass of dried barley straw (g)}} \times 100 \quad (1)$$

160
$$\text{SR yield (wt\%)} = \frac{\text{mass of SR obtained (g)}}{\text{mass of dried barley straw (g)}} \times 100 \quad (2)$$

161 **2.4 Design of experiments**

162 CCD is one of the most commonly used RSM designs for investigating the
163 synergistic effect of different variables on a target parameter. In this study, the
164 experimental design with 4 variables and 3 levels was employed to optimize the HTL
165 of barley straw process conditions using Design Expert 9.0.3 software based on the
166 response value (BO yield) obtained in the experiments. Four variables were reaction
167 temperature (X_1), reaction time (X_2), catalyst dosage (X_3) and biomass/water mass
168 ratio (X_4). Based on the preliminary single factor experiments (Zhu et al., 2015a; Zhu
169 et al., 2015b; Zhu et al., 2014), the range of each value was chosen in the range of
170 260-340 °C, 5-25 min, 2-18 wt% and 9-21wt% respectively, as shown in Table 2. The
171 design contained a total of 30 experiments, with 16 factorial design, 8 axial points,
172 and 1 center point with 6 replicates to ensure the accuracy of the experiment. Herein,
173 the factorial design was to estimate the curvature for the model. The center point
174 offered a method for estimating the experimental errors and testing lack of fit.

175 The data was analyzed using Design Expert 9.0.3 and Minitab 18 software,
176 optimizing the BO yield in this process. The analysis of variance (ANOVA) and
177 significance test of the BO yield obtained under different operating conditions were
178 carried out in order to evaluate the quality of the model fitting, while the residual
179 analysis was performed to assess model adequacy. The quadratic polynomial equation
180 was used to study the effects of the linear, square terms and interacting terms of the
181 independent variables, as is shown in Eq. (3).

182
$$Y = a_0 + \sum_{i=1}^4 a_i X_i + \sum_{i=1}^4 a_{ii} X_i^2 + \sum_{i=1}^4 \sum_{i < j} a_{ij} X_i X_j \quad (3)$$

183 where Y is the response function (BO yield), X_1 , X_2 , X_3 and X_4 are the reaction
 184 temperature, reaction time, catalyst dosage and biomass/water mass ratio, respectively;
 185 a_0 is intercept of model, a_i , a_{ii} , a_{ij} represents the coefficients of linear, quadratic
 186 and interaction terms, respectively.

187

188 **Table 2** Experimental variables and levles

Variables		Level of variables				
		-2	-1	0	1	2
X_1	reaction temperature (°C)	260	280	300	320	340
X_2	reaction time (min)	5	10	15	20	25
X_3	catalyst dosage ^a (wt%)	2	6	10	14	18
X_4	biomass/water mass ratio (wt%)	9	12	15	18	21

189 ^a based on dry biomass

190 2.5 Characterization of BO

191 The elemental composition were determined using a 2400 Series II CHNS/O
 192 element analyzer (PerkinElemer, USA). Duplicate analysis of each element was
 193 conducted, and the mean value were presented here.

194 Higher heating values of BO were calculated according to Dulong formula, due
 195 to the fact that the BO collected in micro reactors was not enough for test.

196
$$\text{HHV}(\text{MJ/kg}) = 0.3383C + 1.422(H - O/8) \quad (4)$$

197 Where C, H, O represents the mass percentage of carbon, hydrogen and oxygen
 198 content, respectively.

199 The chemical composition of BO was analyzed on CLARUS SQ 8 Gas
 200 Chromatograph/Mass Spectrometer (GC/MS) from PerkinElmer. Before test, the
 201 samples were dried at 105 °C for 24 hours, and trimethylsilyl derivatization was
 202 applied so as to enhance the volatility of samples. The resulting silylated derivatives
 203 were diluted with 2.0 mL of hexane and subjected to a fixed temperature ramping
 204 profile: 75 °C (held 2 min) → 250 °C at a rate of 20 °C/min (held 10 min). The

205 compounds were identified using NIST 2011 spectrum library.

206 3. Results and Discussion

207 3.1 RSM results and response surface analysis

208 3.1.1 Model fitting

209 The experimental conditions and the response value (BO yield) are shown in
210 Table 3. As shown in Table 3, the BO yield varied between 22.12 wt% and 37.64 wt%
211 at different liquefaction conditions. The highest BO yield was obtained at a
212 temperature of 300 °C, 15min, with addition of 10% catalyst and biomass/water ratio
213 of 21%. The fitting quadratic equation for BO yield is determined based on these data,
214 as shown in Eq. (3).

$$\begin{aligned} Y = & 34.9717 + 1.75X_1 + 0.286667X_2 + 1.42583X_3 + 1.65083X_4 - 0.4125X_1X_2 + 0.815X_1X_3 \\ & - 0.9325X_1X_4 - 0.23125X_2X_3 - 0.02625X_2X_4 - 0.25625X_3X_4 - 2.34X_1^2 - 0.29125X_2^2 \\ & - 1.5375X_3^2 - 0.53X_4^2 \end{aligned}$$

215
216 (3)

217 The ANOVA was performed and the results are shown in Table 4. It was found
218 that the model was highly significant with p-value <0.0001. The lower the p-value,
219 the more significant the factor. Thus, the model was suitable for this experiment. In
220 addition, the p-value of “lack of fit” was 0.0723 (p > 0.05), indicating that lack of fit
221 was insignificant, which implied that the proposed model fit the data well. The
222 quadratic polynomial regression model for BO yield showed that factor of X₁, X₃, X₄,
223 the interaction term of X₁X₃, X₁X₄, and quadratic term of X₁², X₃² were significant,
224 suggesting that the response was interactive and complicated. Besides, a high
225 coefficient of determination value (R²=0.9262) was obtained, which indicated that the
226 model can predict the experimental data effectively.

Table 3 CCD matrix, actual product yield and properties of BO

Run	variables				BO yield(wt%)	SR yield(wt%)	Elemental composition (wt%)				HHV(MJ/kg)
	reaction temperature(° C)	reaction time(min)	catalyst dosage (wt%)	biomass/water mass ratio (wt%)			C	H	N	O	
1	300	15	10	15	34.97±0.79	15.87±3.13	68.25	7.43	0.68	23.64	29.45
2	280	10	6	12	24.13±3.59	21.93±2.94					
3	320	20	14	18	33.99±2.18	18.91±1.21	69.21	7.21	0.71	22.87	29.60
4	320	10	6	12	28.85±1.59	12.75±2.41	67.94	6.89	0.75	24.42	28.44
5	300	15	10	15	34.97±0.79	15.87±3.13					
6	300	15	10	15	34.97±0.79	15.87±3.13					
7	300	5	10	15	32.78±2.56	17.86±1.98	68.08	7.13	0.78	24.01	28.90
8	320	20	6	12	27.88±1.59	15.12±1.85	68.78	7.45	0.73	23.04	29.77
9	300	15	18	15	32.62±1.59	17.27±1.76	67.27	6.84	0.73	25.16	28.01
10	280	10	14	12	26.14±0.85	24.97 ±2.11					
11	300	15	2	15	27.12±3.02	18.21±3.03	65.46	6.66	0.76	27.12	26.80
12	300	15	10	15	34.97±0.79	15.87±3.13					
13	280	20	6	12	25.14±1.24	23.18 ±1.64					
14	280	20	14	12	27.73±1.89	23.98 ±1.97					
15	280	20	14	18	29.97±0.97	24.99±2.43					

16	300	25	10	15	36.93±0.53	19.91±1.54	65.50	7.19	0.72	26.59	27.66
17	320	10	6	18	29.91±1.70	18.17±2.05	66.91	7.63	0.78	24.68	29.10
18	280	10	14	18	31.74±1.63	25.79±2.51					
19	300	15	10	15	34.97±0.79	15.87±3.13					
20	280	10	6	18	29.73±1.74	24.45±1.89					
21	320	20	14	12	31.83±2.17	18.45±2.72	67.98	7.96	0.72	23.34	30.17
22	320	10	14	18	34.24±0.58	18.71±2.68	68.28	7.19	0.69	23.84	29.09
23	300	15	10	9	30.16±0.93	17.38±2.49	67.92	7.53	0.91	23.64	29.48
24	300	15	10	15	34.97±0.79	15.87±3.13					
25	260	15	10	15	22.12±1.48	27.63±1.90					
26	320	10	14	12	33.96±0.94	14.31±2.79	67.36	7.12	0.67	24.85	28.50
27	320	20	6	18	29.25±1.66	18.25±2.84	68.14	7.23	0.75	23.88	29.09
28	340	15	10	15	31.20±1.83	19.12±3.13	69.31	7.33	0.72	22.64	29.85
29	300	15	10	21	37.64±0.69	17.26±2.99	68.83	7.09	0.82	23.26	29.23
30	280	20	6	18	31.49±1.77	28.34±1.09					

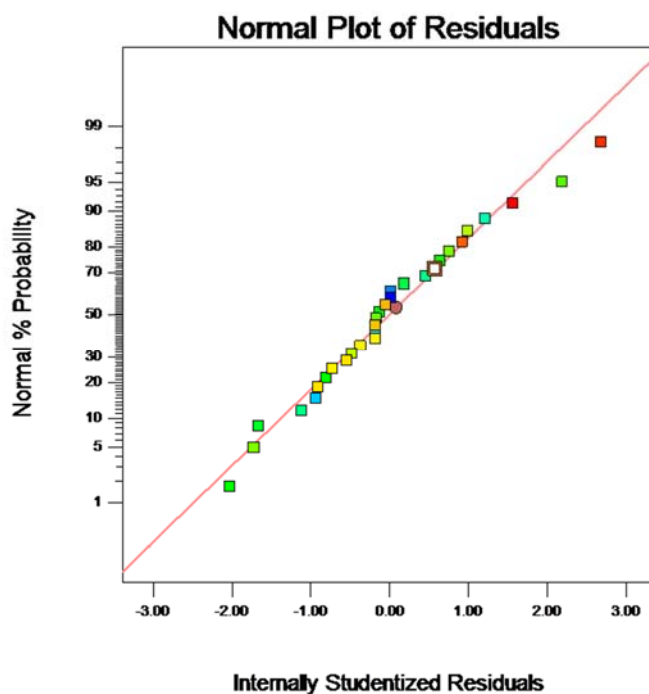
Table 4 ANOVA of the RSM model for BO yield

Sources	Sum of squares	Degree of freedom	Mean square	F-value	P-value	Remarks
Model	410.77	14	29.34	13.45	<0.0001	Significant
X_1	73.50	1	73.50	33.69	<0.0001	Significant
X_2	1.97	1	1.97	0.90	0.3568	
X_3	48.79	1	48.79	22.36	0.0003	Significant
X_4	65.41	1	65.41	29.98	<0.0001	Significant
X_1X_2	2.72	1	2.72	1.25	0.2816	
X_1X_3	10.63	1	10.63	4.87	0.0433	Significant
X_1X_4	13.91	1	13.91	6.38	0.0233	Significant
X_2X_3	0.86	1	0.86	0.39	0.5406	
X_2X_4	0.011	1	0.011	5.053E-003	0.9443	
X_3X_4	1.05	1	1.05	0.48	0.4983	
X_1^2	150.19	1	150.19	68.83	<0.0001	Significant
X_2^2	2.23	1	2.23	1.07	0.3181	
X_3^2	64.84	1	64.84	29.72	<0.0001	Significant
X_4^2	7.70	1	7.70	3.53	0.0798	
Residual	32.73	15	2.18			
Lack of fit	29.03	10	2.90	3.92	0.0723	Not significant
Pure error		3.70	5	0.74		
Total		443.50	29			
R^2		0.9262				

229 3.1.2 Diagnostics and validation of model

230 To study the appropriateness of the model, the diagnostic plots such as normal
231 plot and predicted vs. actual were developed. Figs. 2-3 illustrate the normal
232 probability and residual plot of model for BO yield. The internally studentized
233 residual is calculated by the division of residual to its standard deviation, which is
234 used to estimate the error varying between points. Typically, each point on normal
235 probability plot should lie approximately in a straight line, thus it can be inferred that
236 the estimated effects are the real (Box and Draper, 2007). As observed in Fig. 2, the
237 plotted data formed a straight line roughly, so the residuals for BO yield fitted normal

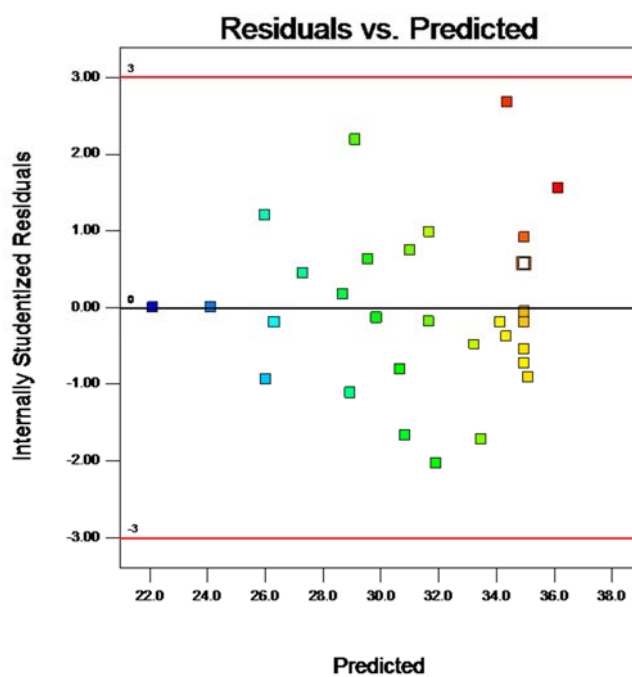
238 distribution and the model was proved in good agreement with experimental data. In
239 addition, the residual plot shown in Fig. 3 revealed that the residual of BO yield had a
240 random scatter, therefore, no outlier points were detected.



241

242

Fig. 2. Normal probability plot for BO yield.



243

244

Fig. 3. Residual vs. predicted values for BO yield.

245 **3.1.3 Response surface plots and optimization**

246 Three dimensional response surface and contour plots for BO yield based on
247 reaction temperature, reaction time, catalyst dosage, biomass/water mass ratio were
248 plotted in Figs. 4-9. Since there are four factors in this study, each time the other two
249 factors were fixed at their level “0” when plotting two factors. As illustrated in figures,
250 all the curve shape of response surfaces are downwards convex, with a central point in
251 the studied range, indicating that there is a maximum response for BO yield.

252 Fig. 4 shows the effect of reaction temperature and time on BO yield. The rate of
253 the BO yield with temperature was greater than that of time, indicating that BO yield
254 depended more on temperature than on time. This observation was consistent with
255 findings reported in the literature (Chan et al., 2017; Gollakota et al., 2017; Jindal and
256 Jha, 2016). The BO yield increased sharply as reaction temperature increased from
257 280 to 310 °C, which was higher than 35.3 wt% when the temperature was between
258 305 and 309 °C and time was between 15 and 17.3 min. When barley straw was
259 treated at low temperature (at 260 °C in run 25), the bond cleavage among different
260 components could not be completely finished, at the same time reactions such as
261 hydrolyzation and depolymerization leading to smaller molecules could not be
262 finished. With increasing in temperature, the dehydration, decarboxylation,
263 dehydroxylation reactions between macromolecules formed by initial reactions
264 occurred and therefore BO containing various organic compounds (phenolics, organic
265 acids, aromatic hydrocarbons) identified in Table 5, SR, gases were formed at
266 relatively higher temperature. Further increase in temperature (>310 °C), the yield of
267 BO gradually decreased, accompanied by an increase in SR yield shown in Table 3.
268 The reduction could be explained by the polymerization/condensation of phenols and
269 their derivatives, which were unstable to form solid products at high temperatures, as
270 evidenced by the decreased phenolics content in Fig. 10.

271 The effect of reaction temperature and catalyst dosage on BO yield is shown in
272 Fig. 5. It showed that increase in both two independent variables enhanced the BO
273 yield initially, but then slowly declined. There was an optimum point for temperature
274 at around 308 °C and catalyst dosage of 12.4 %. According to our previous study,

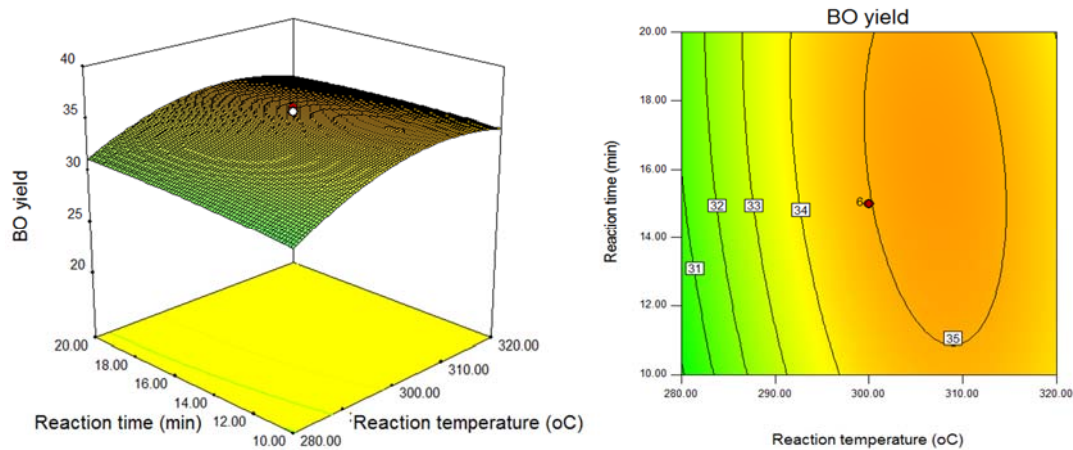
275 K_2CO_3 employed in a fixed concentration during HTL of barley straw changed
276 reaction pathway where more phenolic compounds were formed in BO (Zhu et al.,
277 2015b). Further increase in catalyst dosage at a fixed temperature gave insignificant
278 influence on BO yield owing to the desired reactions such as
279 decomposition/depolymerization were inhibited. Similar finding that optimal BO
280 yield and energy recovery were obtained when a suitable catalyst amount was used
281 during HTL of birch sawdust (Malins, 2017).

282 Fig. 6 illustrates the effect of reaction temperature and biomass/water ratio on
283 BO yield. The BO yield increased with increasing temperature when it was below 305
284 °C at a fixed biomass/water ratio. Afterwards a slight decrease in BO yield was
285 observed, which might be due to gasification of oily compounds or
286 polymerization/condensation reactions mentioned above. It is evidenced that
287 biomass-to-solvent ratio strongly affects BO and SR yield. When water was employed
288 in HTL, it serves as both a solvent and hydrogen donor for hydrolyzing the molecules
289 and therefore biomass/water ratio is a key parameter (Anastasakis and Ross, 2011;
290 Cao et al., 2017). In Fig. 6, it can be observed that higher BO yield was reached
291 utilizing appropriate biomass/water ratio (14.5-17%). Due to the role of water
292 involved in the depolymerization reaction, much higher biomass/water ratio resulted
293 in lower solubility of small molecular products or intermediates in water, and
294 inhibited the formation of oily products.

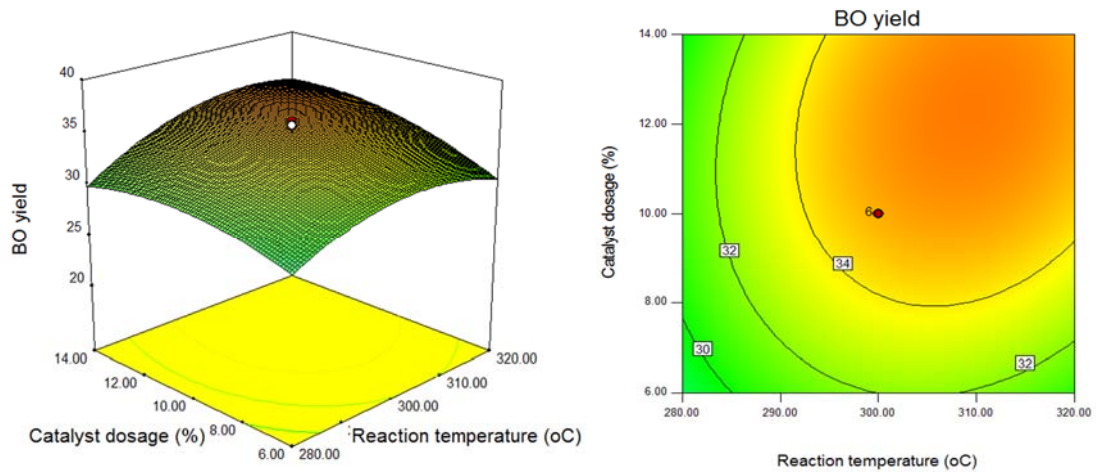
295 The effect of reaction time and catalyst dosage on BO yield is depicted in Fig. 7.
296 It can be observed that the effect of time was closely linked to catalyst dosage. More
297 specifically, the BO yield showed no remarkable change with lower catalyst dosage
298 (less than 8%). It increased as catalyst dosage increased from 8 to 13.6%, and then
299 became nearly stationary. Maximum BO yield (35.3 wt%) was obtained when the
300 catalyst content was between 11.2% and 12.3% and the time ranged from 15 to 18.3
301 min. Most importantly, when the catalyst dosage was above 10% and reaction time
302 was longer than 15 min, both of two variables had no apparent impact on the BO yield,
303 which was higher than 35 wt%. This implied that too short a reaction time was not
304 enough for the BO formation, while too long may result in the SR formation as shown

305 in Table 3 or gas formation from cracking of liquid products as pointed by Xu et al.
306 (Xu and Etcheverry, 2008).

307 Fig. 8 shows the effect of reaction time and biomass/water ratio on BO yield. As
308 it is clear from this figure, higher BO yield was obtained at higher biomass/water ratio,
309 which exceeded 35wt% when biomass/water ratio was above 16.2%. A further
310 increase of this ratio caused insignificant changes in BO yield, the reasons of which
311 have already been explained above in Fig. 6. While, the influence of reaction time on
312 BO yield was relatively insignificant compared with the catalyst dosage and
313 biomass/water ratio, as seen from Figs. 7 and 8. Therefore, it provided some guidance
314 for the choice of important parameters in HTL of straw in continuous plant in the
315 future. The effect of catalyst dosage and biomass/water ratio on BO yield is depicted
316 in Fig. 9. It was observed that BO yield increased with biomass/water at a fixed
317 catalyst dosage. This result indicated that the range of biomass/water ratio involved in
318 this study was suitable for depolymerization reaction and BO formation. Higher BO
319 yield appeared when the catalyst content was higher than 8.2% and biomass/water
320 ratio was above 15%.

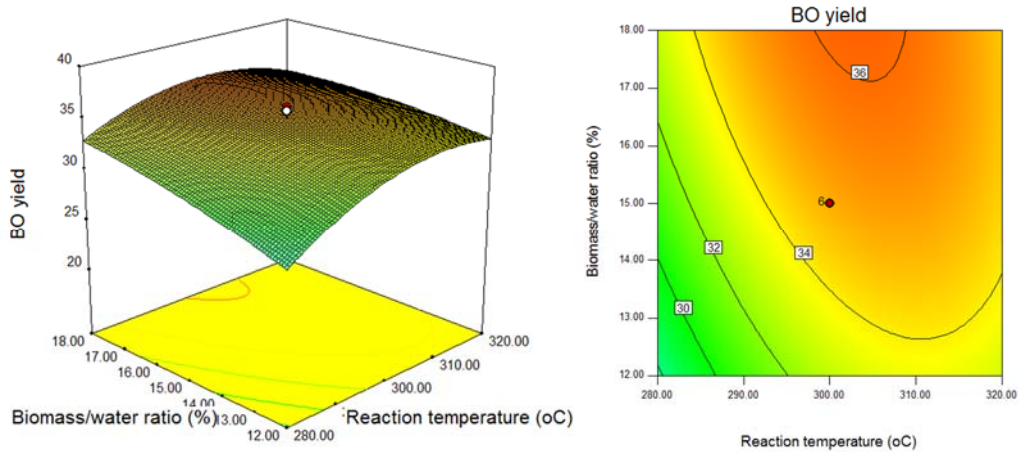


321
322 **Fig. 4** The response surface (a) and contour plots (b) for BO yield as a function of
323 temperature (°C) and reaction time (min).



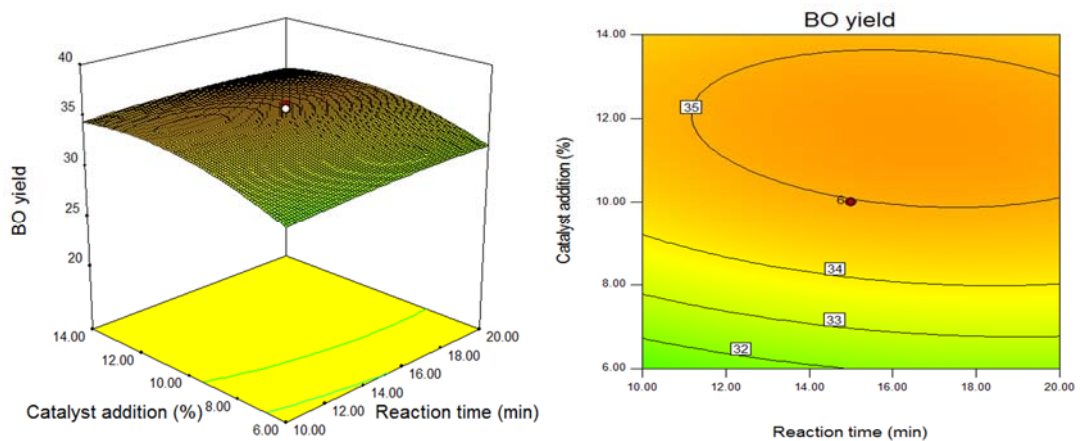
324

325 **Fig. 5** The response surface (a) and contour plots (b) for BO yield as a function of
 326 temperature (°C) and catalyst dosage (%).



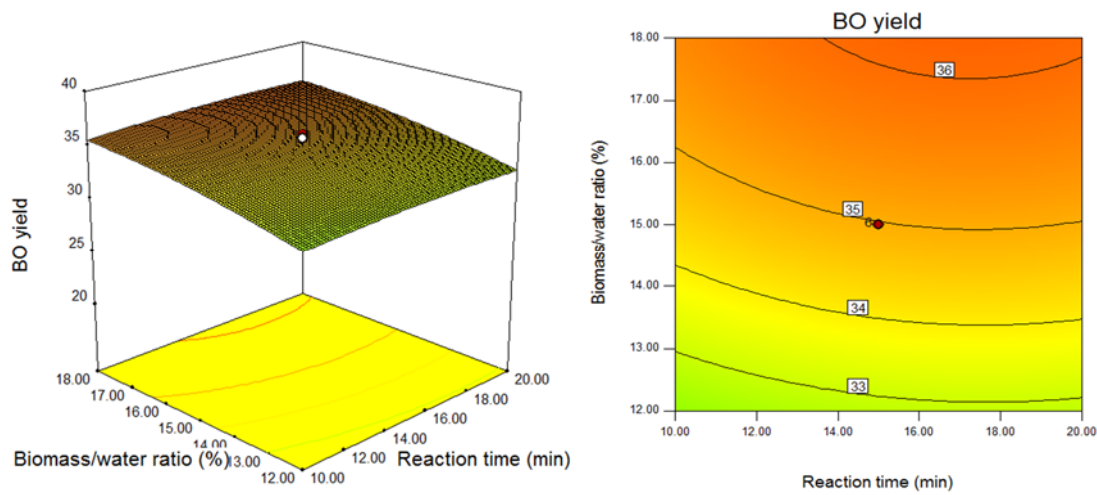
327

328 **Fig. 6** The response surface (a) and contour plots (b) for BO yield as a function of
 329 temperature (°C) and biomass/water ratio (%).

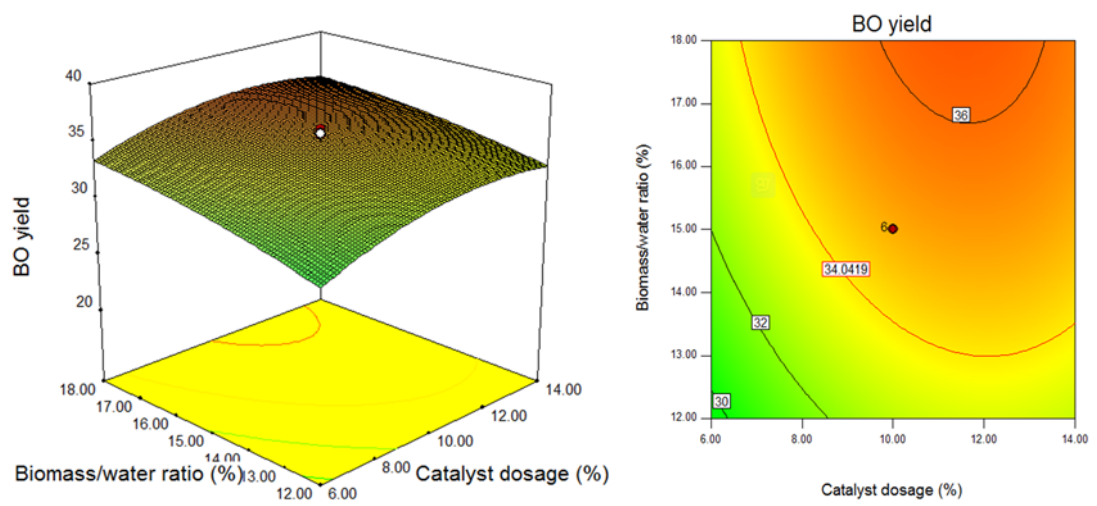


330

331 **Fig. 7** The response surface (a) and contour plots (b) for BO yield as a function of
 332 reaction time (min) and catalyst dosage (%).



333
 334 **Fig. 8** The response surface (a) and contour plots (b) for BO yield as a function of
 335 reaction time (min) and biomass/water ratio (%).



336
 337 **Fig. 9** The response surface (a) and contour plots (b) for BO yield as a function of
 338 catalyst dosage(%) and biomass/water ratio.

339 The optimum values of the process variables for the maximum BO yield are
 340 shown in Table 4. Higher biomass content was chosen for optimal utilization of waste,
 341 with a biomass/water ratio of 18.0 applied in optimization process. Confirmatory
 342 experiments were carried out three times under the predicted optimal condition in
 343 order to verify the predicted optimization result. It showed that the experimental BO
 344 yield closely agreed with model prediction value, with the error of 6.25. Therefore,
 345 RSM is a powerful tool for optimizing the operational conditions of BO production
 346 from barley straw.

347 **Table 4** Optimum operating conditions, predicted and experimental BO yield

Optimum operating conditions				BO yield (wt%)		Error ^a
Reaction temperature (°C)	Reaction time (min)	Catalyst dosage (%)	Biomass/water ratio	Predicted	Experimental	(%)
304.8	15.5	11.7	18.0	36.46	38.72±0.36	6.25

348 ^a Error=(Experimental BO yield –Predicted BO yield)/ Predicted BO yield

349 **3.2 Chemical compositions of BO**

350 The elemental composition and HHV of BO are shown in Table 3. Herein BO
 351 obtained at 280 °C were not analyzed due to lower amount of BO yield, which is not
 352 anticipated in HTL process. According to Table 3, the carbon content was between
 353 65.46% and 69.31%. Increasing the temperature led to a higher carbon content, while
 354 it showed no remarkable change on the hydrogen content (about 7%). In contrast, a
 355 prolonged reaction time or reduced catalyst dosage reduced carbon content in BO,
 356 which could be considered when optimizing HTL process. The HHV range from
 357 26.80 and 30.17 MJ/kg.

358 BO obtained from barley straw is a very complex mixture. The chromatograms
 359 of BO are provided as supplementary material. Table 5 shows the organic compounds
 360 in BO at different operating conditions, and only the compounds with high content
 361 were listed here. Most components in BO were volatilized and detected due to the
 362 derivatization before GC/MS analysis. The relative contents of each compound
 363 determined by peak areas ratio were listed as well. Distribution of key groups of
 364 chemical compounds in BO obtained at different reaction conditions is presented in
 365 Fig. 10. As observed, the BO mainly consist of organic acids, phenols and their
 366 derivatives, aromatic hydrocarbons, ketones, aldehydes, alcohols and N-contained
 367 organic compounds. BO produced at lower temperature (300 °C) had higher phenolic
 368 compounds, lower long chain carboxylic acids and lower aromatics than that obtained
 369 at higher temperature (340 °C), while BO obtained from higher temperature was more
 370 complicated compare to lower temperature.

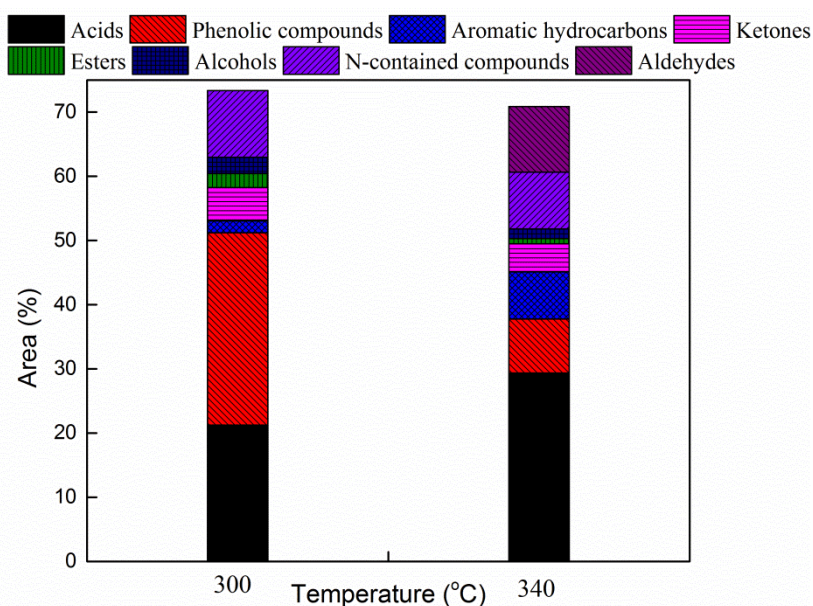
371 **Table 5** Major organic compounds in the BO at different reaction conditions.

Peak	RT	Name of compound	Area (%)
------	----	------------------	----------

	(min)		O-300	O-340
1	3.48	2-Hydroxypropanoic acid	2.95	
2	3.60	1-(3-methylbutyl)-2,3,4,6-tetramethylbenzene	1.85	
3	4.02	Propanoic acid, 2-hydroxy-2-methyl	2.60	
4	4.18	Oenantholacton	1.08	
5	4.59	2,4-Hexadienoic acid, 1-methylethyl ester	1.12	
6	4.78	2-Methoxy phenol	2.19	
7	4.85	2,4-Dimethylphenol	1.58	0.82
8	5.16	Glycerol	1.41	
9	5.18	Phenol, 4-ethyl-2-methoxy-		0.67
10	5.44	1,3-Benzenediol	4.02	2.37
11	5.94	9,10-Anthracenedione, 1,4-dihydroxy-2,3-		1.79
12	5.96	3,5-Dimethylphenol	2.90	
13	5.96	.Alpha.-methylstilbene		2.09
14	6.01	2,6-Dimethoxyphenol	11.62	3.51
15	6.10	2,4-Dihydroxybutanoic acid	1.43	
16	6.39	Methylhydroquinone	3.58	
17	6.39	Fluorene		4.46
18	6.42	[1,1'-Biphenyl]-4-ol, 3,5-Bis(1,1-dimethylethyl)-		1.04
19	6.54	2,6-Dimethoxy-1-hydroxy-phenate butyl	4.07	
20	6.54	Noscapine		2.88
21	6.67	5,8-Dimethoxy-1,4-dimethyl-1,4-dihydro-2,3-quinoxalin edithione		0.97
22	6.70	1-Naphthalenol, 2-[(4-chlorophenyl)azo]	2.32	
23	6.83	2'-Hydroxypropiophenone		1.08
24	6.88	1,3-Dimethyl-6-ethyl-5-[(3-(2-acetamido-3-oxo-3-methoxy)propyl)indol-2-yl]-uracil		1.70
25	6.96	3,4-Dimethoxybenzoic acid	2.13	1.59
26	7.08	1,3,5-Benzenetricarboxylic acid, trimethyl ester		0.83
27	7.4	9,10-Anthracenedione, 1,4-diamino-		0.65
28	7.48	(1E)-1-Phenyl-1-hepten-3-ol		1.49
29	7.74	Albomaculine		0.96
30	7.93	Oxazolidine-2,4-dione, 5-[4-(ethylmethylamino)phenyl]-		0.92
31	7.96	Ethanone, 1-[4-(4-morpholybenzylidenami	1.60	
32	7.99	Xylitol	1.11	
33	8.08	5,6,7,8-Tetrahydro-3-nitronaphthalen-2-ol-1-carboxylic acid, met		0.79
34	8.21	2,5-Cyclohexadien-1-one, 2,5-dimethyl-4-[(2,4,5-trimethylphenyl)]imi	5.11	
35	8.44	1,5-Diphenyl-3-styryl-2-pyrazolin	1.35	
36	8.44	Benzene, (2-methyl-1-propenyl)-		0.79
37	8.52	Tetradecanoic acid		4.26
38	8.53	2H,8H-Benzo[1,2-B:5,4-B']Dipyran-2-one, 5-methoxy-8,8-dimethyl- 10-(3-methyl-2-butenyl)-	5.20	

39	8.8	Albomaculine		1.50
40	9.49	Hexadecanoic acid	7.28	16.91
41	10.27	Oleic acid	2.32	4.45
42	10.37	Octadecanoic acid	0.78	1.45
43	10.60	Benzyl ether	0.57	
44	10.90	Cyclopropaneoctanal, 2-octyl-		10.18
45	13.03	Azelaic acid		0.70
46	13.05	9,12,15-Octadecatrienoic acid	1.17	
Total			73.34	70.84

372



373

374 **Fig. 10** Distribution of key chemical compounds in BO obtained at different
 375 reaction conditions. (left: 300 °C, 15min, 10wt% catalyst and 15% biomass/water
 376 ratio. right: 340 °C, 15min, 10wt% catalyst and 15% biomass/water ratio.)

377 Phenols and their derivatives mainly contained 2,6-dimethoxyphenol,
 378 1,3-benzenediol, methylhydroquinone, 3,5-dimethylphenol, 2-methoxy phenol,
 379 2,4-dimethylphenol in BO produced at 300 °C, accounting for 29.96% of detected
 380 compounds. Higher phenolic compounds in BO makes it a promising material in the
 381 applications of either as a phenol substitute in bio-phenolic resins or bio-fuel. While
 382 their contents decreased or even disappeared at 340 °C. Phenol derivatives could be
 383 originated from cleavage of ether bonds or C-C linkage in lignin (Jindal and Jha,
 384 2016), dehydration of furfurals during the degradation of cellulose or
 385 dehydrogenation of aldehydes/acids (Nazem and Tavakoli, 2017). At higher
 386 temperature, reactions such as hydrogenolysis, dehydrogenation and

387 dehydroaromatization may occur and therefore convert some phenolics to
388 hydrocarbons (Cheng et al., 2017). This led to the decreased contents of phenolic
389 compounds together with higher aromatic hydrocarbons content increasing from 1.85%
390 at 300 °C to 7.34% at 340 °C. The presence of fluorine and benzene,
391 (2-methyl-1-propenyl)- in BO at 340 °C supported this statement.

392 Different types of organic acids were also detected in BO, most of which were
393 long chain fatty acids. They mainly consist of hexadecanoic acid, oleic acid and
394 octadecanoic acid, all of which increased when raising the temperature. Total organic
395 acids accounted for 29.36% at 340 °C. Short chain fatty acids such as
396 2-hydroxypropanoic acid and propanoic acid, 2-hydroxy-2-methyl can only be found
397 in BO at 300 °C. They were formed by the complex hydrolysis and dehydration
398 reactions of the cellulose, hemicellulose and some extractives fraction in barley straw
399 (Sun et al., 2011). BO obtained under this condition may have the potential to be
400 converted into biodiesel. It should be noted that presence of organic acids would have
401 an adverse effect in storage, transportation and catalytic upgrading (Mortensen et al.,
402 2011).

403 Cyclic ketones, esters, and alcohols were observed in both BO. They were
404 supposed to be derived from the decomposition of cellulose and hemicellulose
405 components (Huber et al., 2006). As pointed by Chen et al., the ketones could
406 transform between organic acids and alcohols due to their instability under HTL
407 conditions(Chen et al., 2014). Table 5 also showed that BO contained small amounts
408 of N-contained compounds, most probably due to the interaction between hydrolysis
409 products from barley straw to form N-containing ring compounds via Mailard
410 reaction (Kruse et al., 2007). Some of the identified compounds in BO are valuable
411 for the chemical industry, which should be further treated according to its application.

412 **4 Conclusions**

413 A five-level CCD selected as a RSM for experiment design was employed to
414 optimize the effect of influencing factors on BO production from HTL of barley straw.
415 Four factors including reaction temperature (X_1), reaction time (X_2), catalyst dosage
416 (X_3) and biomass/water ratio (X_4) were investigated. The ANOVA of quadratic model

417 revealed that BO yield was affected by reaction temperature, catalyst dosage and
418 biomass/water ratio significantly. Besides, the influences of interaction of X_1X_3 and
419 X_1X_4 were more significant. The optimum reaction conditions for the BO production
420 were: a temperature of 304.8 °C, a time of 15.5 min, a biomass/water ratio of 18% and
421 a catalyst content of 11.7 %. The maximum BO yield was 38.72 wt% was obtained
422 under optimum conditions. The experimental data are in good agreement with
423 predicted values, indicating the accuracy of quadratic model for optimization of HTL
424 of barley straw. GC/MS analysis showed that BO mainly contained organic acids,
425 phenols and their derivatives, aromatic hydrocarbons, ketones, aldehydes, alcohols
426 and N-contained organic compounds. The HHV of BO range from 26.80 and 30.17
427 MJ/kg, which has the potential to be used as a potential source of renewable fuel.

428

429 **Acknowledgements**

430 This research was financially supported by FLEXIfuel (DSF-BENMI grant no
431 10-094552). Zhe Zhu thanks the China Scholarship Council for the financial support.

432

433 **References**

- 434 Anastasakis K, Ross AB. Hydrothermal liquefaction of the brown macro-alga *Laminaria Saccharina*:
435 Effect of reaction conditions on product distribution and composition. *Bioresource*
436 *Technology* 2011; 102: 4876-4883.
- 437 Box GEP, Draper NR. *Response Surfaces, Mixtures, and Ridge Analyses*, 2nd Edition. New Jersey: John
438 Wiley & Sons, Inc., 2007.
- 439 Cao L, Zhang C, Chen H, Tsang DCW, Luo G, Zhang S, et al. Hydrothermal liquefaction of agricultural
440 and forestry wastes: state-of-the-art review and future prospects. *Bioresource Technology*
441 2017; 245: 1184-1193.
- 442 Chan YH, Quitain AT, Yusup S, Uemura Y, Sasaki M, Kida T. Optimization of hydrothermal liquefaction of
443 palm kernel shell and consideration of supercritical carbon dioxide mediation effect. *The*
444 *Journal of Supercritical Fluids* 2017.
- 445 Chen W-T, Zhang Y, Zhang J, Yu G, Schideman LC, Zhang P, et al. Hydrothermal liquefaction of
446 mixed-culture algal biomass from wastewater treatment system into bio-crude oil.
447 *Bioresource Technology* 2014; 152: 130-139.
- 448 Cheng S, Wei L, Julson J, Kharel PR, Cao Y, Gu Z. Catalytic liquefaction of pine sawdust for biofuel
449 development on bifunctional Zn/HZSM-5 catalyst in supercritical ethanol. *Journal of*
450 *Analytical and Applied Pyrolysis* 2017; 126: 257-266.
- 451 Déniel M, Haarlemmer G, Roubaud A, Weiss-Hortala E, Fages J. Bio-oil Production from Food
452 Processing Residues: Improving the Bio-oil Yield and Quality by Aqueous Phase Recycle in

453 Hydrothermal Liquefaction of Blackcurrant (*Ribes nigrum* L.) Pomace. *Energy & Fuels* 2016;
454 30: 4895-4904.

455 Das O, Sarmah AK. Value added liquid products from waste biomass pyrolysis using pretreatments.
456 *Science of The Total Environment* 2015; 538: 145-151.

457 Denmark S. StatBank Denmark, 2014.

458 Diamond WJ. *Practical Experiment Design for Engineers and Scientists: Lifetime Learning Publications*,
459 1981.

460 Eriksson L, Johansson E, Kettaneh-Wold N, Wikström C, Wold S. *Design of Experiments Principles and*
461 *Applications*. Umeå, Sweden: Umetrics AB, 1996.

462 Gollakota ARK, Kishore N, Gu S. A review on hydrothermal liquefaction of biomass. *Renewable and*
463 *Sustainable Energy Reviews* 2017.

464 Hassan SNAM, Ishak MAM, Ismail K. Optimizing the physical parameters to achieve maximum
465 products from co-liquefaction using response surface methodology. *Fuel* 2017; 207: 102-108.

466 Hsieh D, Capareda S, Placido J. Batch Pyrolysis of Acid-Treated Rice Straw and Potential Products for
467 Energy and Biofuel Production. *Waste and Biomass Valorization* 2015; 6: 417-424.

468 Hu Y, Feng S, Yuan Z, Xu C, Bassi A. Investigation of aqueous phase recycling for improving bio-crude oil
469 yield in hydrothermal liquefaction of algae. *Bioresource Technology* 2017; 239: 151-159.

470 Huber GW, Iborra S, Corma A. Synthesis of transportation fuels from biomass: chemistry, catalysts, and
471 engineering. *Chemical Reviews* 2006; 106: 4044-4098.

472 IEA. *Energy Statistics*, 2012.

473 Jindal MK, Jha MK. Effect of process parameters on hydrothermal liquefaction of waste furniture
474 sawdust for bio-oil production. *RSC Advances* 2016; 6: 41772-41780.

475 Kruse A, Maniam P, Spieler F. Influence of Proteins on the Hydrothermal Gasification and Liquefaction
476 of Biomass. 2. Model Compounds. *Industrial & Engineering Chemistry Research* 2007; 46:
477 87-96.

478 Kummamuru B. *Global bioenergy statistics 2017*, 2017.

479 Li X, Wang B, Wu S, Kong X, Fang Y, Liu J. Optimizing the Conditions for the Microwave-Assisted
480 Pyrolysis of Cotton Stalk for Bio-Oil Production Using Response Surface Methodology. *Waste*
481 *and Biomass Valorization* 2017; 8: 1361-1369.

482 Liu J, Zhuang Y, Li Y, Chen L, Guo J, Li D, et al. Optimizing the conditions for the microwave-assisted
483 direct liquefaction of *Ulva prolifera* for bio-oil production using response surface
484 methodology. *Energy* 2013; 60: 69-76.

485 Malins K. Production of bio-oil via hydrothermal liquefaction of birch sawdust. *Energy Conversion and*
486 *Management* 2017; 144: 243-251.

487 Midgett JS, Stevens BE, Dassey AJ, Spivey JJ, Theegala CS. Assessing Feedstocks and Catalysts for
488 Production of Bio-Oils from Hydrothermal Liquefaction. *Waste and Biomass Valorization* 2012;
489 3: 259-268.

490 Mortensen PM, Grunwaldt JD, Jensen PA, Knudsen KG, Jensen AD. A review of catalytic upgrading of
491 bio-oil to engine fuels. *Applied Catalysis A: General* 2011; 407: 1-19.

492 Nazem MA, Tavakoli O. Bio-oil production from refinery oily sludge using hydrothermal liquefaction
493 technology. *The Journal of Supercritical Fluids* 2017; 127: 33-40.

494 Parsa M, Jalilzadeh H, Pazoki M, Ghasemzadeh R, Abduli M. Hydrothermal liquefaction of *Gracilaria*
495 *gracilis* and *Cladophora glomerata* macro-algae for biocrude production. *Bioresource*
496 *Technology* 2018; 250: 26-34.

497 Patel B, Guo M, Chong C, Sarudin SHM, Hellgardt K. Hydrothermal upgrading of algae paste: Inorganics
498 and recycling potential in the aqueous phase. *Science of The Total Environment* 2016; 568:
499 489-497.

500 Sander B. Properties of Danish biofuels and the requirements for power production. *Biomass and*
501 *Bioenergy* 1997; 12: 177-183.

502 Suárez-Iglesias O, Urrea JL, Oulego P, Collado S, Díaz M. Valuable compounds from sewage sludge by
503 thermal hydrolysis and wet oxidation. A review. *Science of the Total Environment* 2017;
504 584-585: 921-934.

505 Sun P, Heng M, Sun S-H, Chen J. Analysis of liquid and solid products from liquefaction of paulownia in
506 hot-compressed water. *Energy Conversion and Management* 2011; 52: 924-933.

507 Toor SS, Rosendahl L, Rudolf A. Hydrothermal liquefaction of biomass: A review of subcritical water
508 technologies. *Energy* 2011; 36: 2328-2342.

509 Xiu S, Shahbazi A. Bio-oil production and upgrading research: A review. *Renewable and Sustainable*
510 *Energy Reviews* 2012; 16: 4406-4414.

511 Xu C, Etcheverry T. Hydro-liquefaction of woody biomass in sub- and super-critical ethanol with
512 iron-based catalysts. *Fuel* 2008; 87: 335-345.

513 Xu L, Jiang Y, Wang L. Thermal decomposition of rape straw: Pyrolysis modeling and kinetic study via
514 particle swarm optimization. *Energy Conversion and Management* 2017; 146: 124-133.

515 Younas R, Hao S, Zhang L, Zhang S. Hydrothermal liquefaction of rice straw with NiO nanocatalyst for
516 bio-oil production. *Renewable Energy* 2017; 113: 532-545.

517 Yu KL, Lau BF, Show PL, Ong HC, Ling TC, Chen W-H, et al. Recent developments on algal biochar
518 production and characterization. *Bioresource Technology* 2017.

519 Zhang B, von Keitz M, Valentas K. Thermochemical liquefaction of high-diversity grassland perennials.
520 *Journal of Analytical and Applied Pyrolysis* 2009; 84: 18-24.

521 Zhu Z, Rosendahl L, Toor SS, Yu D, Chen G. Hydrothermal liquefaction of barley straw to bio-crude oil:
522 Effects of reaction temperature and aqueous phase recirculation. *Applied Energy* 2015a; 137:
523 183-192.

524 Zhu Z, Toor S, Rosendahl L, Yu D, Chen G. Influence of alkali catalyst on product yield and properties
525 via hydrothermal liquefaction of barley straw. *Energy* 2015b; 80: 284-292.

526 Zhu Z, Toor SS, Rosendahl L, Chen G. Analysis of product distribution and characteristics in
527 hydrothermal liquefaction of barley straw in sub- and supercritical water. *Environmental*
528 *Progress & Sustainable Energy* 2014; 33: 737-743.

529